

Quantum Chemistry Study of Uranium(VI), Neptunium(V), and Plutonium(IV,VI) Complexes with Preorganized Tetradentate Phenanthrolineamide Ligands

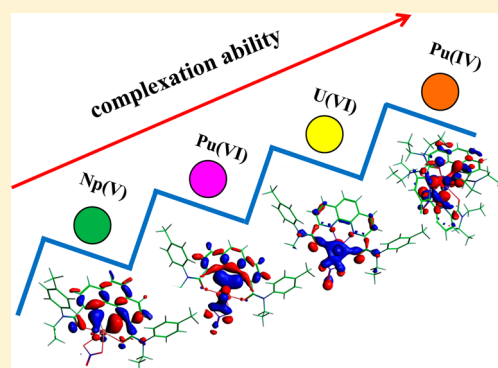
Cheng-Liang Xiao,^{†,‡} Qun-Yan Wu,^{†,‡} Cong-Zhi Wang,[†] Yu-Liang Zhao,[†] Zhi-Fang Chai,^{*,†,§} and Wei-Qun Shi^{*,†}

[†]Key Laboratory of Nuclear Radiation and Nuclear Energy Technology and Key Laboratory for Biomedical Effects of Nanomaterials and Nanosafety, Institute of High Energy Physics, Chinese Academy of Sciences, Beijing 100049, China

[§]School for Radiological and Interdisciplinary Sciences (RAD-X) and Collaborative Innovation Center of Radiation Medicine of Jiangsu Higher Education Institutions, Soochow University, Suzhou 215123, China

Supporting Information

ABSTRACT: The preorganized tetradentate 2,9-diamido-1,10-phenanthroline ligand with hard–soft donors combined in the same molecule has been found to possess high selectivity toward actinides in an acidic aqueous solution. In this work, density functional theory (DFT) coupled with the quasi-relativistic small-core pseudopotential method was used to investigate the structures, bonding nature, and thermodynamic behavior of uranium(VI), neptunium(V), and plutonium(IV,VI) with phenanthrolineamides. Theoretical optimization shows that Et-Tol-DAPhen and Et-Et-DAPhen ligands are both coordinated with actinides in a tetradentate chelating mode through two N donors of the phenanthroline moiety and two O donors of the amide moieties. It is found that $[\text{AnO}_2\text{L}(\text{NO}_3)]^{n+}$ ($\text{An} = \text{U}^{\text{VI}}, \text{Np}^{\text{V}}, \text{Pu}^{\text{VI}}; n = 0, 1$) and $\text{PuL}(\text{NO}_3)_4$ are the main 1:1 complexes. With respect to 1:2 complexes, the reaction $[\text{Pu}(\text{H}_2\text{O})_9]^{4+}(\text{aq}) + 2\text{L}(\text{org}) + 2\text{NO}_3^-(\text{aq}) \rightarrow [\text{PuL}_2(\text{NO}_3)_2]^{2+}(\text{org}) + 9\text{H}_2\text{O}(\text{aq})$ might be another probable extraction mechanism for Pu^{IV} . From the viewpoint of energy, the phenanthrolineamides extract actinides in the order of $\text{Pu}^{\text{IV}} > \text{U}^{\text{VI}} > \text{Pu}^{\text{VI}} > \text{Np}^{\text{V}}$, which agrees well with the experimental results. Additionally, all of the thermodynamic reactions are more energetically favorable for the Et-Tol-DAPhen ligand than the Et-Et-DAPhen ligand, indicating that substitution of one ethyl group with one tolyl group can enhance the complexation abilities toward actinide cations (anomalous aryl strengthening).



1. INTRODUCTION

The design of selective ligands toward specific metal ions is determined by many factors, such as the chelate ring size, the hard–soft acid–base theory, and preorganization.^{1–4} Among these factors, preorganization has been of considerable interest. A so-called preorganized ligand is one that requires the lowest energy to complex a target guest ion or molecule. Quantities of preorganized ligands, such as cyclodextrins,⁵ crown ethers,⁶ cryptands,⁷ calixarenes,^{8–10} and pillararenes,^{11–14} have been reported to possess excellent host–guest properties. Recently, 1,10-phenanthroline-2,9-dicarboxylic acid (PDA),^{15–18} 2,9-bis-(hydroxymethyl)-1,10-phenanthroline (PDALC),^{19–21} 1,10-phenanthroline-2,9-dicarboxamide (PDAM),^{22,23} and 2,9-dipyrid-2-yl-1,10-phenanthroline (DPP)^{24–27} tetradentate ligands (Figure 1) have received much attention because of their extraordinary properties in complexing metal ions. It is worth mentioning that Hancock and his co-workers have harvested meaningful both experimental and theoretical results in this area.^{1–3,15–23,25–27}

As shown in Figure 1, all of these ligands have a preorganized phenanthroline skeleton with N or O donors decorated in the 2

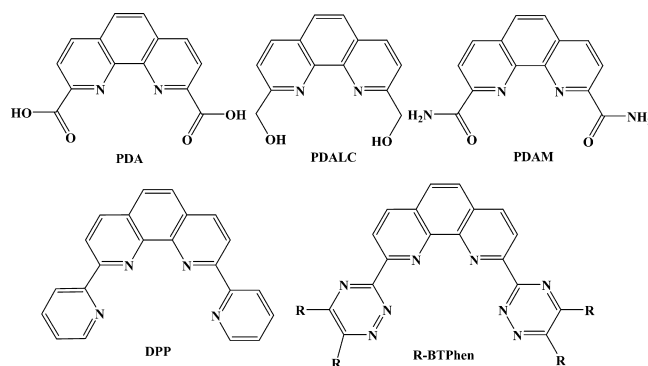


Figure 1. Chemical structures of preorganized tetradentate phenanthroline-derived ligands in previous work.

and 9 positions. Such a phenanthroline backbone behaves like a rigid cleft, which controls metal-ion-size-based selectivity.

Received: April 7, 2014

Published: September 30, 2014

Additionally, the phenanthroline moiety is locked by integrated benzo rings, which benefits thermodynamic stabilization by avoiding σ -bond rotation in their bipyridine analogues.^{4,28} Interestingly, these tetradentate phenanthroline-derived ligands were found to have a strong ability to complex a relatively large metal with an ionic radius close to 1.0 Å.^{17,22,27} One of the important applications of these preorganized ligands might be use in the separation of actinides from an acidic aqueous solution in that the sizes of most of actinides are around 1.0 Å.^{4,18,28–35}

A type of preorganized tetradentate N-heterocyclic ligand, 2,9-bis(1,2,4-triazin-3-yl)-1,10-phenanthroline (BTPhen; Figure 1), was reported by Harwood et al.^{29–31,34,35} to achieve a rapid and efficient separation of minor actinides from lanthanides in a highly acidic solution. Meanwhile, the withdrawing effect of triazine rings of BTPhen results in lower pK_a (3.1) compared to that of the phenanthroline itself (4.9),²⁹ which can reduce the extent of protonation and hydrolysis in a HNO₃ solution. The PDAM ligand (Figure 1),^{22,23} having both hard O and soft N donors, is particularly interesting because of its extremely low pK_a value (0.6) and promising complexation ability toward almost all actinide ions. On the basis of the PDAM structure, Galletta et al.³⁶ synthesized the 2,9-bis[(*N,N*-dioctylamino)-carbonyl]-1,10-phenanthroline ligand and found that it possessed separation ability of minor actinide from lanthanides with $SF_{Am/Eu}$ of ~ 40 in the presence of a synergistic agent (Br-Cosan). Additionally, Charbonnel et al.³⁷ also designed a new kind of phenanthrolineamide by grafting one or two amide groups onto a 2,9-dipyridyl-1,10-phenanthroline skeleton, aiming at the separation of all of the actinides over lanthanides. To further improve the distribution ratios and selectivities of such ligands toward all of the actinides, we have reported a novel tetradentate phenanthroline-derived ligand, Et-Tol-DAPhen (Figure 2), which exhibited excellent separation

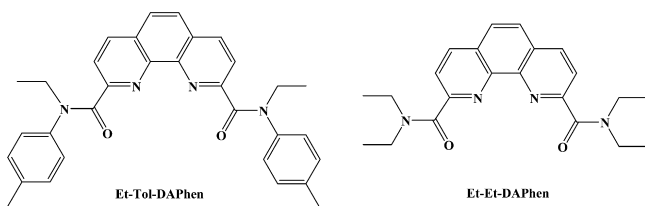


Figure 2. Chemical structures of the Et-Tol-DAPhen and Et-Et-DAPhen ligands studied in this work.

ability toward nearly all of the actinides [actinide(III, IV,VI)] from an acidic aqueous solution.³⁸ The separation factors of thorium(IV), uranium(VI), and americium(III) toward europium(III) are 2277, 277, and 67 in 1.0 M HNO₃, respectively. Nevertheless, because of the radiotoxicity-induced experimental difficulties, up to now, systematic investigations on the extraction of plutonium and neptunium cations with phenanthrolineamides are still lacking. It is highly desirable to disclose the coordination modes and thermodynamic behaviors of plutonium and neptunium with phenanthrolineamides, which might help to predict the extraction abilities of phenanthrolineamides toward plutonium and neptunium cations.

In this work, density functional theory (DFT) coupled with the quasi-relativistic small-core pseudopotential method was performed to explore the complexation behavior of uranium(VI), neptunium(V), and plutonium(IV,VI) with phenanthro-

lineamides. At first, we explored the probable actinide species in water and a nitrate solution. Then, the structures of actinide complexes with phenanthrolineamides as well as their bonding character were studied. Next, the effects of the starting species, nitrate anions, and solvent effect on the probable complexation reactions of phenanthrolineamides with actinides were also elucidated. In addition, the complexation properties of two phenanthrolineamides, Et-Tol-DAPhen and Et-Et-DAPhen (Figure 2), were theoretically compared to give more insight for understanding the mechanisms behind the selectivity and hence to shed light on the design of highly efficient ligands for actinides.

2. THEORETICAL METHODS

All of the theoretical calculations were carried out using the DFT method with the *Gaussian 09* package.³⁹ The functional we used is B3LYP, which combines the Becke 88 exchange functional and the three-parameter functional (B3)⁴⁰ with the Lee, Yang, and Parr (LYP)⁴¹ correlation functional. For U, Np, and Pu atoms, scalar relativistic effects were taken into consideration, with the quasi-relativistic effective core potentials (RECPs)^{42,43} replacing 60 core electrons. Corresponding ECP60MWB-SEG valence basis sets⁴⁴ were used to describe the remaining valence electrons. Spin-orbit effects were neglected in this work. With regard to the ligands, the standard Pople-style polarized valence triple- ξ 6-311G(d,p) basis set was used for C, H, O, and N atoms. We have extensively tested different hybrid functionals of DFT and found that the B3LYP/RECP method was reliable in the theoretical calculations of actinides ions and their complexes with organic ligands.^{45–49}

All of the complexes were optimized at the B3LYP/6-311G(d,p)/RECP level of theory in the gas phase. Harmonic vibrational frequencies were calculated at the same level of theory to verify the minimum character of the optimized structures on the potential energy surfaces. The natural atomic charges and Wiberg bond indices (WBIs)⁵⁰ were calculated by natural bond orbital (NBO)^{51,52} analyses with the same method. The frequencies of all of the chemical species were calculated at the same level of theory on the basis of the optimized geometries. The enthalpy (H), Gibbs free energy (G), and binding energy (E) with zero-point-energy (ZPE) and thermal corrections were calculated with the same method in the gas phase (298.15 K, 0.1 MPa). Solvation effects were considered by the conductor-like screening model (COSMO) approach⁵³ to yield the solvation energy based on the optimized structures in the gas phase. In addition, there is little effect on the solvation energies if we reoptimize the structures in aqueous solution. In order to confirm the reliabilities of the structures and energies in aqueous solution, we reoptimize the structures of $[AnO_2L]^{n+}$ ($n = 1$ and 2 ; An = U, Np, and Pu; L = Et-Tol-DAPhen) as examples in water solution. The optimized structural parameters for the gas phase and aqueous solution, respectively, as well as the solvent energies are provided in Table S1 in the Supporting Information (SI). It can be clearly observed that the bond lengths for the gas phase and aqueous solution are almost the same, and the largest difference is only 0.02 Å. The solvent energies based on the optimized structure in the gas phase and aqueous solution are also similar with the largest difference of 0.94 kcal/mol. Moreover, the relative solvent energies are in the same trend based on the optimized structures in the gas phase and aqueous solution. Therefore, on the basis of the results of structural parameters and solvent energies, the effects of

solution on the structures and energies are negligible, which are in excellent agreement with previous conclusions.^{54,55} Thus, single-point calculations were verified to minimize computational costs without sacrificing much accuracy in the solvation energies. In this work, solvent effects were considered on the basis of single-point calculations at the same level of theory using the COSMO model in water and cyclohexanone, respectively.

3. RESULTS AND DISCUSSION

3.1. Actinide Structures in Water and Nitrate Solution.

In this work, comprehensive characterization of stable uranium(VI), neptunium(V), and plutonium(IV,VI) complexes with water and nitrate ions was performed using the B3LYP/6-311G(d,p)/RECP level of theory. Although some structures have been optimized using the B3LYP/6-31G(d) basis set in our previous work,⁴⁸ systematic analyses and comparisons of these stable species with experimental data are still lacking.

As we know, the most stable species of uranium are in the form of U^{VI}, and the pentacoordinated [UO₂(H₂O)₅]²⁺ is the dominant species in aqueous solution.⁵⁶ The optimized structure of [UO₂(H₂O)₅]²⁺ (Figure 3) exhibits C₅ symmetry

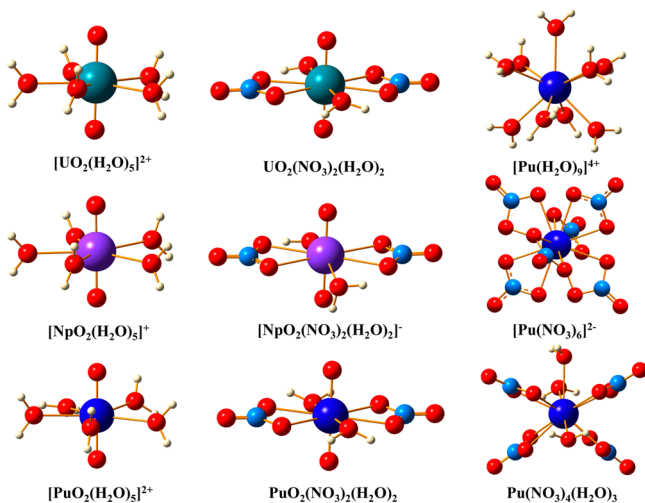


Figure 3. Optimized uranium(VI), neptunium(V), and plutonium(IV,VI) structures with water and nitrate ions in the gas phase. Green, purple, blue, red, sky blue, and white colors represent U, Np, Pu, O, N, and H atoms, respectively.

with average bond lengths of 2.49 and 1.75 Å for U–O and U=O (Table 1), respectively. Compared to the available experimental parameters, B3LYP/6-311G(d,p)/RECP gives rather reasonable structural results with an average error of 0.05 Å. Likewise, the neptunium(V) and plutonium(VI) analogues possess similar geometries and acceptable errors. In the presence of nitrate ions, UO₂²⁺, NpO₂⁺, and PuO₂²⁺ are in favor of coordination with nitrate anions in a bidentate mode (Figure 3). Both of the UO₂²⁺ and PuO₂²⁺ cations are energetically stable in the neutral state upon complexation with nitrate anions and water molecules. Two nitrate anions and two water molecules are involved in the complexation to reach the maximum coordination number of U^{VI} and Pu^{VI}. On the experimental side, in the crystal structure of UO₂(NO₃)₂(H₂O)₂, the nitrate anions are coordinated with an average U–O_N bond distance of 2.50 Å, while the water molecules are coordinated with a U–O_W bond distance of 2.48

Table 1. Selected Average Bond Lengths (Å) for Uranium(VI), Neptunium(V), and Plutonium(IV,VI) Structures with Water and Nitrate Ions Calculated by the B3LYP Method in Comparison with the Experimental Data (in Parentheses)

species	An–O _W (H ₂ O)	An– O _N (NO ₃ [–])	An=O	average error
[UO ₂ (H ₂ O) ₅] ²⁺	2.49 (2.41) ⁵⁶		1.75 (1.76)	0.05
[NpO ₂ (H ₂ O) ₅] ⁺	2.48 (2.40) ⁵⁶		1.79 (1.81)	0.05
[PuO ₂ (H ₂ O) ₅] ²⁺	2.49 (2.41) ⁵⁹		1.77 (1.75)	0.05
UO ₂ (NO ₃) ₂ (H ₂ O) ₂	2.53 (2.45) ⁵⁷	2.48 (2.50)	1.77 (1.75)	0.04
[NpO ₂ (NO ₃) ₂ (H ₂ O) ₂] [–]	2.70 (–)	2.61 (–)	1.81 (–)	
PuO ₂ (NO ₃) ₂ (H ₂ O) ₂	2.51 (2.43) ⁵⁸	2.48 (2.50)	1.79 (1.73)	0.05
[Pu(H ₂ O) ₉] ⁴⁺	2.45 (2.39) ⁶⁰			0.06
[Pu(NO ₃) ₆] ^{2–}		2.52 (2.48) ⁶⁰		0.04
Pu(NO ₃) ₄ (H ₂ O) ₃	2.56 (2.38) ⁶⁰	2.46 (2.46)		0.05

Å.⁵⁷ Additionally, Gaunt et al.⁵⁸ isolated the crystals of PuO₂(NO₃)₂(H₂O)₂ from an aqueous solution of Pu^{VI} in nitric acid after slow evaporation. The average bond lengths of Pu–O_W, Pu–O_N, and Pu=O are 2.43, 2.50, and 1.73 Å, respectively. As shown in Table 1, both of the theoretical results of UO₂(NO₃)₂(H₂O)₂ and PuO₂(NO₃)₂(H₂O)₂ are in good agreement with the experimental data (average errors of 0.04 and 0.05 Å, respectively). However, no analogous neptunium(V) nitrate structure was reported for comparison with the optimized one. According to our previous calculations,⁴⁸ we can see that the anionic [NpO₂(NO₃)₂(H₂O)₂][–] species, similar to UO₂(NO₃)₂(H₂O)₂ and PuO₂(NO₃)₂(H₂O)₂, is more energetically favorable than the neutral NpO₂(NO₃)(H₂O)₄ in the gas phase. With respect to Pu^{IV}, the bond length of Pu–O_W in [Pu(H₂O)₉]⁴⁺ is a little bit (0.06 Å) longer than that obtained from the extended X-ray absorption fine structure (EXAFS) technique.⁵⁹ In addition, the tetranitrate and hexanitrate complexes of plutonium(IV) are known to be the dominant species in acidic aqueous nitrate solutions. All of the nitrate anions in the optimized [Pu(NO₃)₆]^{2–} and Pu(NO₃)₄(H₂O)₃ structures are coordinated with Pu^{IV} in a bidentate mode. According to the EXAFS results of Allen et al.,⁶⁰ the bond lengths of Pu–O_N are 2.46 and 2.48 Å for Pu(NO₃)₄(H₂O)₃ and [Pu(NO₃)₆]^{2–} species in the nitric acid solution, respectively. It can be seen from Table 1 that the calculated values (2.46 and 2.48 Å) are quite consistent with the experimental ones. Thus, the computational method of B3LYP/6-311G(d,p)/RECP that we selected for modeling uranium(VI), neptunium(V), and plutonium(IV,VI) species is reliable and is therefore used for the calculations of all of the actinide complexes discussed in the following sections. Interestingly, it should be noted that the bond lengths of all of the equatorial An–O_W bonds are overestimated compared to the experimental values,^{54,55} which might be due to the dispersion corrections.

3.2. Uranium(VI), Neptunium(V), and Plutonium(IV,VI) Complexes with DAPhen Ligands. **3.2.1. Geometric Structures.** Initially, the structures of 1:1 types of uranium(VI), neptunium(V), and plutonium(IV,VI) complexes with the Et-Tol-DAPhen and Et-Et-DAPhen ligands were optimized

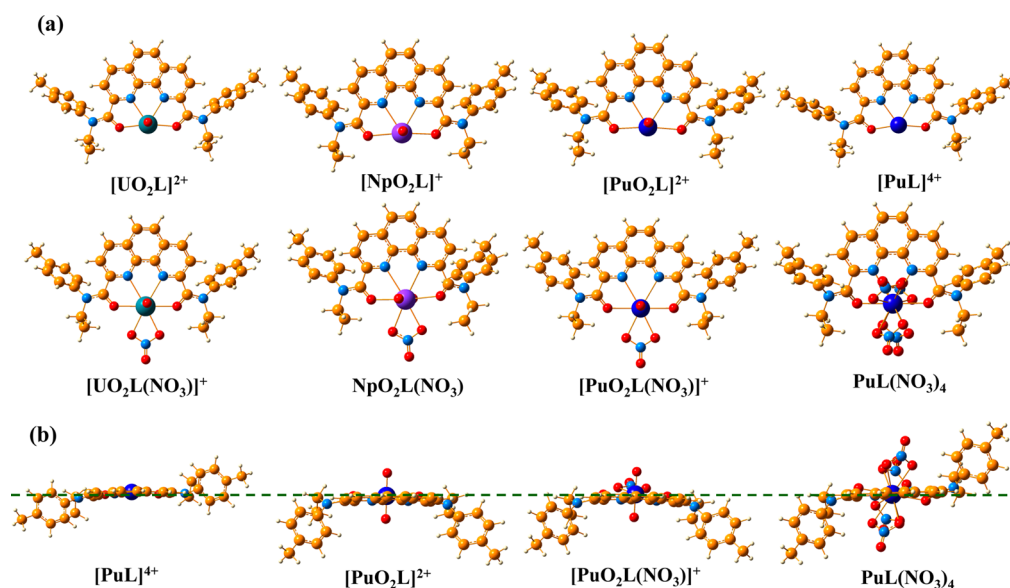


Figure 4. Optimized structures of the actinide complexes with L = Et-Tol-DAPhen (1:1 type). Green, purple, blue, orange, red, sky blue, and white colors represent U, Np, Pu, C, O, N, and H atoms, respectively.

Table 2. Selected Bond Lengths (Å) for the Structures of the Actinide Complexes with Et-Tol-DAPhen/Et-Et-DAPhen (1:1 Type) and WBIs of the An–N and An–OBonds

species	An=O	An–N	An–O	An–O _{nitrate}	$W_{\text{An–N}}$	$W_{\text{An–O}}$
[UO ₂ L] ²⁺	1.76/1.76	2.53/2.54	2.33/2.32		0.38/0.38	0.57/0.57
[UO ₂ L(NO ₃)] ⁺	1.77/1.77	2.72/2.73	2.44/2.44	2.47/2.46	0.33/0.33	0.47/0.47
[NpO ₂ L] ⁺	1.80/1.78	2.61/2.61	2.49/2.48		0.27/0.27	0.32/0.33
NpO ₂ L(NO ₃)	1.81/1.80	2.79/2.82	2.61/2.58	2.55/2.54	0.23/0.22	0.28/0.30
[PuO ₂ L] ²⁺	1.77/1.77	2.60/2.56	2.50/2.41		0.26/0.30	0.28/0.37
[PuO ₂ L(NO ₃)] ⁺	1.79/1.79	2.72/2.72	2.47/2.44	2.46/2.45	0.29/0.29	0.37/0.40
[PuL] ⁴⁺		2.49/2.55	2.26/2.23		0.24/0.22	0.38/0.38
PuL(NO ₃) ₄		2.69/2.73	2.49/2.46	2.47/2.51	0.34/0.32	0.41/0.42

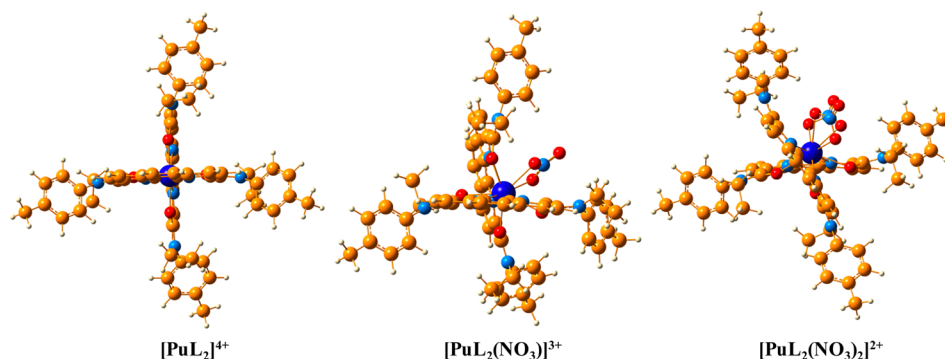


Figure 5. Optimized structures of the plutonium(IV) complexes with Et-Tol-DAPhen (1:2 type). Blue, orange, red, sky blue, and white colors represent Pu, C, O, N, and H atoms, respectively.

(Figures 4 and S1 in the SI). The corresponding selected bond lengths are summarized in Table 2. For all of the complexes, the Et-Tol-DAPhen and Et-Et-DAPhen ligands are both coordinated in a tetradentate chelating mode through two N donors of the phenanthroline moiety and two O donors of the amide moieties. There is not much difference in the structures of the Et-Tol-DAPhen and Et-Et-DAPhen complexes with actinides.

In the absence of nitrate anions, the bond lengths of An–O and An–N in [NpO₂L]⁺ and [PuO₂L]²⁺ species are longer than those of [UO₂L]²⁺, which might be due to the disparities of their ionic radii. The ionic radius of U^{VI} is a bit smaller than

those of Np^V and Pu^{VI}. The involvement of nitrate anions in the coordination results in an increase of the bond lengths for all of the complexes. The bond lengths of [UO₂L(NO₃)]⁺ are very similar to those of [PuO₂L(NO₃)]⁺ and shorter than those of NpO₂L(NO₃). Such results may indicate that the affinity between the Et-Tol-DAPhen ligand and U^{VI} is higher than that of Pu^{VI}. Obviously, the bond lengths of Pu–O and Pu–N in PuL(NO₃)₄ are longer than those of [PuL]⁴⁺ because of the involvement of four nitrate anions in the complexation. Interestingly, after coordination with actinide ions and nitrate anions, the orientation of the Et-Tol-DAPhen structure will

change (Figure 4b). In the crystal or optimized structure of the Et-Tol-DAPhen ligand,³⁸ the molecule has near C_2 symmetry with two tolyl groups on one side and two O atoms of the amide moieties on the opposite side. On the contrary, in the plutonium complexes, all of the O atoms of the amide moieties are coordinated in the plane of the phenanthroline moiety. The two tolyl groups of plutonium(IV) complexes are located in the phenanthroline plane on opposite sides, whereas these two tolyl groups are on the same side in the plutonium(VI) complexes. In the case of $[\text{UO}_2\text{L}(\text{NO}_3)]^+$ ($L = \text{Et-Tol-DAPhen}$), the experimental average bond lengths of $\text{U}=\text{O}$ and $\text{U}-\text{O}$ are 1.74 and 2.41 Å,³⁸ respectively, which are in good agreement with the calculated values (1.77 and 2.44 Å). Although we have not obtained the crystal structure of $\text{PuL}(\text{NO}_3)_4$, the optimized structure of $\text{PuL}(\text{NO}_3)_4$ is analogous to the crystal structure of $\text{ThL}(\text{NO}_3)_4$.³⁸

Furthermore, we optimized the geometrical structures of 1:2 type $[\text{PuL}_2]^{4+}$, $[\text{PuL}_2(\text{NO}_3)]^{3+}$, and $[\text{PuL}_2(\text{NO}_3)_2]^{2+}$ complexes with DAPhen ligands (Figures 5 and S2 in the SI). The Et-Tol-DAPhen and Et-Et-DAPhen complexes with Pu^{IV} exhibit similar geometries. In $[\text{PuL}_2]^{4+}$, the two ligand molecules are in a perpendicular direction to each other. The Pu^{IV} ion is in the center and bound with two N atoms of the phenanthroline moiety and two O atoms of the amide moieties of each ligand. When nitrate anions were involved in the complexation, the coordination number would change from 8 to 10 or 12. The geometrical structures would be much distorted to appropriately adopt the metal cation and nitrate anions at the same time. As shown in Table S2 in the SI, the average bond lengths of $\text{Pu}-\text{N}$ and $\text{Pu}-\text{O}$ become longer after coordination with nitrate anions. The average bond lengths of $\text{Pu}-\text{N}$ and $\text{Pu}-\text{O}$ in $[\text{PuL}_2]^{4+}$ are about 0.06 Å longer those of 1:1 complexes $[\text{PuL}]^{4+}$, which might be due to the steric effect.

3.2.2. Molecular Orbital (MO) and NBO Analysis. To investigate the interactions between U^{VI} , Np^{V} , Pu^{IV} , and Pu^{VI} and the DAPhen ligands, the MOs relevant to the actinides and ligands are displayed in Figures 6 and S3–S6 in the SI. In general, the relatively diffuse 5f orbitals could participate in the chemical bonding for actinide–ligand compounds. The MOs possess σ characters and are mainly contributed by the p atomic orbital of the O/N atom and the f atomic orbital of actinides. In addition, Et-Et-DAPhen and Et-Tol-DAPhen complexes exhibit similar energy levels of MOs. For the 1:1 type complexes, the energy levels of the MOs of neptunium(V) complexes are much higher than those of the uranium(VI) and plutonium(VI) complexes (Figure 6), which indicates relatively weaker affinities between neptunium(V) and ligands than those of uranium(VI) and plutonium(VI) complexes. According to the energy levels of the $[\text{AnO}_2]^{n+}$ ($n = 1, 2$) species, the affinities between the actinides and ligands decrease in the order of $[\text{UO}_2\text{L}(\text{NO}_3)]^+ > [\text{PuO}_2\text{L}(\text{NO}_3)]^+ > \text{NpO}_2\text{L}(\text{NO}_3)$. As for plutonium(IV) complexes, the energy levels of the MOs between plutonium(IV) and ligands are higher compared to those of $[\text{AnO}_2]^{n+}$ ($n = 1, 2$) complexes. In addition, the MO energies of the 1:2 type $[\text{PuL}_2(\text{NO}_3)_2]^{2+}$ complex are in the range of -11.31 to -12.91 eV, which are lower than those of the corresponding MOs in its 1:1 type $\text{PuL}(\text{NO}_3)_4$ complex. This result indicates that the affinities between plutonium(IV) and ligands in 1:2 complexes are stronger than those in 1:1 complexes.

To obtain the bonding character between DAPhen and actinides, NBO analyses of all of the complexes were performed at the B3LYP/6-311G(d,p)/RECP level of theory. As shown in

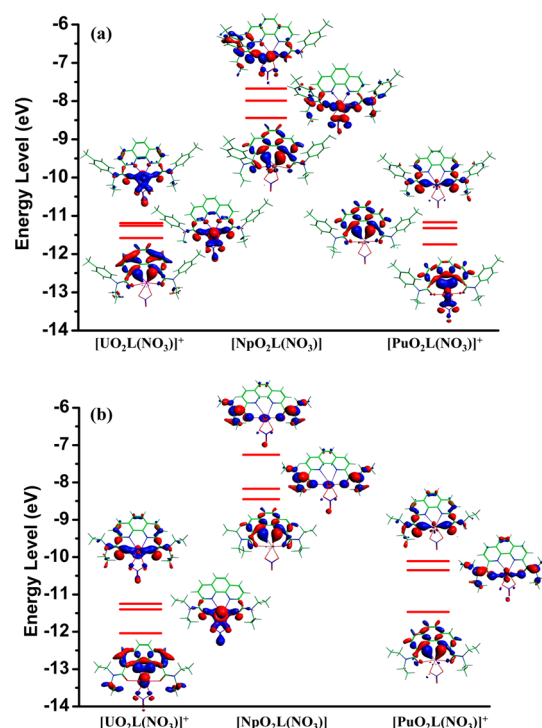


Figure 6. Energy level of α -spin MOs between AnO_2^{n+} ($n = 1, 2$) with $L =$ (a) Et-Tol-DAPhen and (b) Et-Et-DAPhen (1:1 type) and the MO diagrams.

Tables 2 and S2 in the SI, the WBIs of the $\text{An}-\text{N}$ and $\text{An}-\text{O}$ bonds are all in the range of 0.20–0.60, which reveals that the interactions between N/O donors and actinides are weakly covalency. The WBIs of all the bonds in Et-Et-DAPhen complexes are similar to those in Et-Tol-DAPhen. The WBIs of $\text{An}-\text{O}$ bonds are larger than those of $\text{An}-\text{N}$, suggesting more covalency exists in the $\text{An}-\text{O}$ bonds. After coordinated with nitrate anions, the WBIs of $\text{An}-\text{N}$ and $\text{An}-\text{O}$ bonds in uranium(VI) and neptunium(V) complexes become smaller whereas those in plutonium(IV) and plutonium(VI) complexes become larger. In all the 1:1 type complexes containing nitrate anions, the WBIs of $\text{An}-\text{O}$ bonds increase in the following order: $\text{NpO}_2\text{L}(\text{NO}_3) < [\text{PuO}_2\text{L}(\text{NO}_3)]^+ < \text{PuL}(\text{NO}_3)_4 < [\text{UO}_2\text{L}(\text{NO}_3)]^+$. Additionally, it should be noted that the WBIs of 1:2 type plutonium(IV) complexes are relatively larger than their corresponding 1:1 analogues, which suggests that the affinities between N/O donors and Pu^{IV} in 1:2 complexes stronger than those in 1:1 complexes.

The NBO orbital populations of the valence shells of s, p, d, and f are also calculated at the same level of theory. As shown in Tables 3 and S3 in the SI, compared to the $[\text{AnO}_2]^{n+}$ ($n = 1, 2$) species, the corresponding nitrate species have a little higher populations in the s, p, d, and f shells. The occupation numbers of 7s, 7p, and 6d in $[\text{PuL}]^{4+}$ ($L = \text{Et-Tol-DAPhen}$) are only 0.08, 0.07, and 0.37, respectively, which are much smaller than those in $\text{PuL}(\text{NO}_3)_4$. The Et-Et-DAPhen and Et-Tol-DAPhen complexes possess almost the same NBO populations as well as charge distributions (Tables 3 and S2 in the SI). It can be seen that the significant transfer of electrons from ligands to actinide ions results in considerable net charge decreases of the actinide ions and the N/O atoms, suggesting that a strong electron donor–acceptor interaction occurs during the complexation process. In the presence of nitrate anions, the positive charges of the actinide ions in $[\text{AnO}_2]^{n+}$, $[\text{PuL}]^{4+}$, and $[\text{PuL}_2]^{4+}$

Table 3. Calculated NBO Populations (s, p, d, and f) and Natural Charges on the Metal, N, and O Atoms for the Actinide Complexes with Et-Tol-DAPhen/Et-Et-DAPhen (1:1 Type)

species	7s	7p	6d	5f	Q _N	Q _O	Q _M
[UO ₂ L] ²⁺	0.16/0.16	0.25/0.25	1.40/1.40	2.57/2.58	-0.48/-0.47	-0.63/-0.63	1.83/1.83
[UO ₂ L(NO ₃) ₂] ⁺	0.20/0.20	0.40/0.40	1.43/1.43	2.63/2.63	-0.42/-0.42	-0.56/-0.57	1.44/1.44
[NpO ₂ L] ⁺	0.14/0.14	0.23/0.24	1.11/1.13	4.11/4.15	-0.46/-0.45	-0.62/-0.63	1.53/1.50
NpO ₂ L(NO ₃)	0.18/0.18	0.35/0.36	1.16/1.18	4.12/4.15	-0.41/-0.40	-0.55/-0.56	1.23/1.19
[PuO ₂ L] ²⁺	0.15/0.15	0.23/0.23	1.07/1.13	5.27/5.22	-0.45/-0.46	-0.58/-0.61	1.46/1.48
[PuO ₂ L(NO ₃) ₂] ⁺	0.20/0.20	0.38/0.38	1.21/1.22	5.24/5.23	-0.42/-0.42	-0.55/-0.57	1.12/1.12
[PuL] ⁴⁺	0.08/0.07	0.07/0.07	0.37/0.36	5.21/5.16	-0.62/-0.61	-0.81/-0.81	2.26/2.27
PuL(NO ₃) ₄	0.27/0.27	0.56/0.56	1.10/1.10	5.02/5.02	-0.39/-0.38	-0.54/-0.54	0.73/0.74

Table 4. Calculated Changes in the Binding Energies, Enthalpies, and Gibbs Free Energies (kcal/mol) for the Actinide Complexes with Et-Tol-DAPhen/Et-Et-DAPhen (1:1 Type)

reaction	ΔE _g	ΔH _g	ΔG _g	ΔG _{ext}
[UO ₂ (H ₂ O) ₅] ²⁺ + L → [UO ₂ L] ²⁺ + 5H ₂ O	-37.68/-20.01	-35.18/-17.50	-66.75/-49.26	-13.46/-11.25
UO ₂ (NO ₃) ₂ (H ₂ O) ₂ + L → [UO ₂ L] ²⁺ + 2H ₂ O + 2NO ₃ ⁻	272.51/290.17	272.67/290.34	77.07/265.14	22.23/24.44
[UO ₂ (H ₂ O) ₅] ²⁺ + L + NO ₃ ⁻ → [UO ₂ L(NO ₃)] ⁺ + 5H ₂ O	-218.84/-206.34	-215.85/-203.34	-237.33/-224.91	-45.15/-42.17
UO ₂ (NO ₃) ₂ (H ₂ O) ₂ + L → [UO ₂ L(NO ₃)] ⁺ + 2H ₂ O + NO ₃ ⁻	91.34/103.84	91.99/104.50	77.07/89.50	-15.51/-12.53
[NpO ₂ (H ₂ O) ₅] ⁺ + L → [NpO ₂ L] ⁺ + 5H ₂ O	10.36/30.58	11.52/31.67	-15.76/4.49	-13.53/-7.91
[NpO ₂ (NO ₃) ₂ (H ₂ O) ₂] ⁻ + L → [NpO ₂ L] ⁺ + 2H ₂ O + 2NO ₃ ⁻	142.51/162.73	142.64/162.79	119.00/139.25	-3.26/2.35
[NpO ₂ (H ₂ O) ₅] ⁺ + L + NO ₃ ⁻ → NpO ₂ L(NO ₃) + 5H ₂ O	-87.41/-68.96	-85.74/-67.27	-102.98/-84.96	-25.38/-19.12
[NpO ₂ (NO ₃) ₂ (H ₂ O) ₂] ⁻ + L → NpO ₂ L(NO ₃) + 2H ₂ O + NO ₃ ⁻	44.74/63.19	45.38/63.85	31.87/49.89	-15.12/-8.85
[PuO ₂ (H ₂ O) ₅] ²⁺ + L → [PuO ₂ L] ²⁺ + 5H ₂ O	12.55/45.77	14.11/47.26	4.63/37.55	-40.01/-24.16
PuO ₂ (NO ₃) ₂ (H ₂ O) ₂ + L → [PuO ₂ L] ²⁺ + 2H ₂ O + 2NO ₃ ⁻	247.83/281.05	248.23/281.39	222.94/255.86	-9.72/6.13
[PuO ₂ (H ₂ O) ₅] ²⁺ + L + NO ₃ ⁻ → [PuO ₂ L(NO ₃)] ⁺ + 5H ₂ O	-143.58/-129.74	-142.32/-128.14	-141.49/-126.51	-55.88/-43.45
PuO ₂ (NO ₃) ₂ (H ₂ O) ₂ + L → [PuO ₂ L(NO ₃)] ⁺ + 2H ₂ O + NO ₃ ⁻	91.70/105.53	91.80/105.98	76.90/91.88	-25.59/-13.16
[Pu(H ₂ O) ₉] ⁴⁺ + L → [PuL] ⁴⁺ + 9H ₂ O	-80.24/27.91	-61.92/-228.42	-140.87/-61.19	42.96/186.24
[Pu(NO ₃) ₆] ²⁻ + L → [PuL] ⁴⁺ + 6NO ₃ ⁻	884.18/982.33	883.12/716.62	828.80/908.48	147.09/290.37
Pu(NO ₃) ₄ (H ₂ O) ₃ + L → [PuL] ⁴⁺ + 4NO ₃ + 3H ₂ O	866.62/964.76	868.05/701.55	808.21/887.89	120.73/264.00
[Pu(H ₂ O) ₉] ⁴⁺ + L + 4NO ₃ ⁻ → PuL(NO ₃) ₄ + 9H ₂ O	-938.21/-920.81	-929.94/-912.17	-959.00/-944.27	-104.22/-99.31
[Pu(NO ₃) ₆] ²⁻ + L → PuL(NO ₃) ₄ + 2NO ₃ ⁻	16.21/33.61	15.10/32.86	10.68/25.41	-0.09/4.82
Pu(NO ₃) ₄ (H ₂ O) ₃ + L → PuL(NO ₃) ₄ + 3H ₂ O	-1.36/16.04	0.03/17.79	-9.91/4.82	-26.46/-21.55

complexes are much higher than those of their corresponding nitrate complexes.

3.2.3. Energy Analysis. To explore the complexation mechanisms of phenanthrolineamides with actinides, quantities of thermodynamic reactions were simulated at the B3LYP/6-311G(d,p)/RECP level of theory. As shown in Table 4, the choice of starting reactants has a large effect on the reaction energies. The complexation reactions using [AnO₂(H₂O)₅]ⁿ⁺ species as starting reactants are more energetically favorable than those using their corresponding [AnO₂(NO₃)₂(H₂O)₂]ⁿ⁻ (n = 0, 1) species. For example, all of the values of ΔE, ΔH, and ΔG of the reaction of [UO₂(H₂O)₅]²⁺ + L → [UO₂L]²⁺ + 5H₂O are negative, whereas those of the reaction of UO₂(NO₃)₂(H₂O)₂ + L → [UO₂L]²⁺ + 2H₂O + 2NO₃⁻ are positive. Additionally, the energies for forming [AnO₂L(NO₃)]ⁿ⁺ (n = 0, 1) complexes are more negative than those for forming [AnO₂L]ⁿ⁺ (n = 1, 2). For U^{VI}, Np^V, and Pu^{VI}, the reaction of [AnO₂(H₂O)₅]ⁿ⁺ (n = 1, 2) + L + NO₃⁻ → [AnO₂L(NO₃)]ⁿ⁺ (n = 0, 1) + 5H₂O might be dominant in the complexation of phenanthrolineamides with actinides in a nitric acid solution. Thus, we concluded that [AnO₂(H₂O)₅]ⁿ⁺ (n = 1, 2) might be the species in aqueous solution and [AnO₂L(NO₃)]ⁿ⁺ (n = 0, 1) could be the extracted species. For Pu^{IV}, it is also found that using [Pu(H₂O)₉]⁴⁺ instead of [Pu(NO₃)₆]²⁻ or Pu(NO₃)₄(H₂O)₃ species as the starting reactants is more beneficial for the complexation reactions to form 1:1 (Table 4) and 1:2 (Table S4 in the SI) type complexes. Obviously, the

thermodynamic reactions for forming PuL(NO₃)₄ (1:1 type) and [PuL₂(NO₃)₂]²⁺ complexes (1:2 type) possess large energetic advantages. Thus, the reactions of [Pu(H₂O)₉]⁴⁺ + L + 4NO₃⁻ → PuL(NO₃)₄ + 9H₂O and [Pu(H₂O)₉]⁴⁺ + 2L + 2NO₃⁻ → [PuL₂(NO₃)₂]²⁺ + 9H₂O might be the probable 1:1 and 1:2 complexation mechanisms, respectively. In addition, all of the thermodynamic reactions of Et-Tol-DAPhen are more energetically favorable than those of the Et-Et-DAPhen ligand, indicating that substitution of one ethyl group with one tolyl group is better for complexation of the actinide ions. Similar phenomena had already been experimentally observed in bidentate organophosphorus, carbamoylmethylphosphine oxide (CMPO), dipicolinamide, bipyridinediamide, and terpyridinediamide ligands, which is known as the so-called "anomalous aryl strengthening".^{61,62} If we substitute tolyl groups for ethyl groups, the basicities of the O/N donors in the phenanthrolineamides will decrease. However, delocalization of the electron density from tolyl to the C=O group and then to the actinide ions can anomalously enhance stabilization of the actinide–ligand complexes.

To better determine the solvent extraction mechanisms of actinides by phenanthrolineamide ligands, we took the solvent effect into consideration.⁶³ For example, during the solvent extraction of U^{VI} from aqueous solution (aq) to cyclohexanone (org) (ΔG_{ext}), one of the extraction mechanisms can be described as UO₂(NO₃)₂(H₂O)₂(aq) + L(org) → [UO₂L(NO₃)]⁺(org) + 2H₂O(aq) + NO₃⁻(aq) (L = Et-Tol-

DAPhen). As listed in Tables 4 and S4 in the SI, the changes of the Gibbs free energies (ΔG_{org}) in cyclohexanone calculated using the COSMO approach would vary much compared to ΔG_{g} . For example, ΔG_{g} is 77.07 kcal/mol whereas ΔG_{ext} is -15.51 kcal/mol in the complexation reaction of $\text{UO}_2(\text{NO}_3)_2(\text{H}_2\text{O})_2(\text{aq}) + \text{L}(\text{org}) \rightarrow [\text{UO}_2\text{L}(\text{NO}_3)]^+(\text{org}) + 2\text{H}_2\text{O}(\text{aq}) + \text{NO}_3^-(\text{aq})$ ($\text{L} = \text{Et-Tol-DAPhen}$), which suggests that the solvent effect can increase the possibility of this reaction. However, the solvent effect can also result in less possibility for certain reactions, such as $[\text{Pu}(\text{H}_2\text{O})_9]^{4+}(\text{aq}) + \text{L}(\text{org}) \rightarrow [\text{PuL}]^{4+}(\text{org}) + 9\text{H}_2\text{O}(\text{aq})$. Anyway, the relative stabilities do not change upon going from the gas phase to extraction process. Forming nitrate complexes using hydrated actinide cations as the starting reactants is quite favorable. From the viewpoint of energy, the phenanthrolineamides extract actinides in the order of $\text{Pu}^{\text{IV}} > \text{U}^{\text{VI}} > \text{Pu}^{\text{VI}} > \text{Np}^{\text{V}}$. On the experimental side, Lapka et al.⁶⁴ reported that the order of extractability was determined to be $\text{An}^{\text{IV}} > \text{An}^{\text{VI}} > \text{An}^{\text{V}}$ by a diamide of dipicolinic acid extractant in 3.0 M HNO_3 . In addition, *N,N,N',N'*-tetraalkyl-6,6''-(2,2':6',2''-terpyridine)-diamides were found to hold the strongest extraction abilities toward Pu^{IV} among An^{III} , An^{IV} , An^{V} , and An^{VI} ions.⁶² In our previous work,³⁸ it was also observed that the distribution ratios of An^{IV} with Et-Tol-DAPhen extractant in cyclohexanone were higher than those of An^{VI} . In this regard, our calculated results not only agree with previous experimental data but also highlight the importance of starting species, nitrate anions, ligands, and the solvent effect in the extraction process.

4. CONCLUSIONS

In summary, the structures, bonding nature, and thermodynamic behavior of uranium(VI), neptunium(V), and plutonium(IV, VI) complexes with phenanthrolineamides were studied with the quasi-relativistic DFT method in this work. In the optimized structures, actinides are coordinated with phenanthrolineamides through two N donors of the phenanthroline moiety and two O donors of the amide moieties. According to the calculated energies, the complexation reactions with $[\text{AnO}_2(\text{H}_2\text{O})_5]^{n+}$ ($n = 1, 2$) and $[\text{Pu}(\text{H}_2\text{O})_9]^{4+}$ as the starting species are more favorable than those with their corresponding nitrate analogues. Additionally, when the nitrate anions are involved in the complexation process, it is liable to form more stable species. The $[\text{AnO}_2\text{L}(\text{NO}_3)]^{n+}$ ($n = 0, 1$), $\text{PuL}(\text{NO}_3)_4$, and $[\text{PuL}_2(\text{NO}_3)_2]^{2+}$ species might be the most probable complexes in solvent extraction. Furthermore, the complexation abilities between phenanthrolineamides and actinides are in the order of $\text{Pu}^{\text{IV}} > \text{U}^{\text{VI}} > \text{Pu}^{\text{VI}} > \text{Np}^{\text{V}}$, which are quite consistent with the experimental results. Although the structures and bonding character of actinides complexes with Et-Tol-DAPhen and Et-Et-DAPhen ligands are almost the same, all of the thermodynamic reactions are energetically favorable for the Et-Tol-DAPhen ligand, which has been experimentally demonstrated by the so-called "anomalous aryl strengthening". Thus, our predicted results not only agree well with previous experimental data but also highlight the importance of starting species, nitrate anions, ligands, and the solvent effect to determine the complexation abilities of phenanthrolineamides with actinides.

■ ASSOCIATED CONTENT

Supporting Information

Additional optimized structures, α -spin MO diagrams, selected bond lengths, WBIs, natural charges, calculated NBO populations, solvent energies, and the complete *Gaussian 09* reference (ref 39). This material is available free of charge via the Internet at <http://pubs.acs.org>.

■ AUTHOR INFORMATION

Corresponding Authors

*(W.-Q.S) E-mail: shiwq@ihep.ac.cn.

*(Z.-F.C) E-mail: zfchai@suda.edu.cn.

Author Contributions

[‡]These authors contributed equally to this work.

Notes

The authors declare no competing financial interest.

■ ACKNOWLEDGMENTS

This work was supported by the Major Research Plan "Breeding and Transmutation of Nuclear Fuel in Advanced Nuclear Fission Energy System" of the Natural Science Foundation of China (Grants 91326202 and 91126006) and the National Natural Science Foundation of China (Grants 21477130, 11275219, and 21261140335), the "Strategic Priority Research Program" of the Chinese Academy of Sciences (Grant XDA030104), and the China Postdoctoral Science Foundation (Grants 2013M530734 and 2014T70123). This work is also supported by a project funded by the Priority Academic Program Development of Jiangsu Higher Education Institutions. The results described in this work were obtained on the ScGrid of Supercomputing Center, Computer Network Information Center of the Chinese Academy of Sciences.

■ REFERENCES

- (1) Hancock, R. D.; Martell, A. E. *Chem. Rev.* **1989**, *89*, 1875.
- (2) Hancock, R. D.; Melton, D. L.; Harrington, J. M.; McDonald, F. C.; Gephart, R. T.; Boone, L. L.; Jones, S. B.; Dean, N. E.; Whitehead, J. R.; Cockrell, G. M. *Coord. Chem. Rev.* **2007**, *251*, 1678.
- (3) Hancock, R. D. *Chem. Soc. Rev.* **2013**, *42*, 1500.
- (4) de Sahb, C.; Watson, L. A.; Nadas, J.; Hay, B. P. *Inorg. Chem.* **2013**, *52*, 10632.
- (5) Rekharsky, M. V.; Inoue, Y. *Chem. Rev.* **1998**, *98*, 1875.
- (6) Steed, J. W. *Coord. Chem. Rev.* **2001**, *215*, 171.
- (7) Caminade, A. M.; Majoral, J. P. *Chem. Rev.* **1994**, *94*, 1183.
- (8) Wieser, C.; Dieleman, C. B.; Matt, D. *Coord. Chem. Rev.* **1997**, *165*, 93.
- (9) de Namor, A. F. D.; Cleverley, R. M.; Zapata-Ormachea, M. L. *Chem. Rev.* **1998**, *98*, 2495.
- (10) Zhang, Z. X.; Drapailo, A.; Matvieiev, Y.; Wojtas, L.; Zaworotko, M. J. *Chem. Commun.* **2013**, *49*, 8353.
- (11) Ogoshi, T.; Kanai, S.; Fujinami, S.; Yamagishi, T. A.; Nakamoto, Y. *J. Am. Chem. Soc.* **2008**, *130*, 5022.
- (12) Strutt, N. L.; Zhang, H. C.; Giesener, M. A.; Lei, J. Y.; Stoddart, J. F. *Chem. Commun.* **2012**, *48*, 1647.
- (13) Xue, M.; Yang, Y.; Chi, X. D.; Zhang, Z. B.; Huang, F. H. *Acc. Chem. Res.* **2012**, *45*, 1294.
- (14) Yao, Y.; Zhou, Y. J.; Dai, J.; Yue, S. Y.; Xue, M. *Chem. Commun.* **2014**, *50*, 869.
- (15) Melton, D. L.; VanDerveer, D. G.; Hancock, R. D. *Inorg. Chem.* **2006**, *45*, 9306.
- (16) Dean, N. E.; Hancock, R. D.; Cahill, C. L.; Frisch, M. *Inorg. Chem.* **2008**, *47*, 2000.
- (17) Williams, N. J.; Dean, N. E.; VanDerveer, D. G.; Luckay, R. C.; Hancock, R. D. *Inorg. Chem.* **2009**, *48*, 7853.

- (18) Ogden, M. D.; Sinkov, S. I.; Nilson, M.; Lumetta, G. J.; Hancock, R. D.; Nash, K. L. *J. Solution Chem.* **2013**, *42*, 211.
- (19) Gephart, R. T.; Williams, N. J.; Reibenspies, J. H.; De Sousa, A. S.; Hancock, R. D. *Inorg. Chem.* **2008**, *47*, 10342.
- (20) Gephart, R. T.; Williams, N. J.; Reibenspies, J. H.; De Sousa, A. S.; Hancock, R. D. *Inorg. Chem.* **2009**, *48*, 8201.
- (21) Williams, N. J.; Ballance, D. G.; Reibenspies, J. H.; Hancock, R. D. *Inorg. Chim. Acta* **2010**, *363*, 3694.
- (22) Merrill, D.; Hancock, R. D. *Radiochim. Acta* **2011**, *99*, 161.
- (23) Merrill, D.; Harrington, J. M.; Lee, H. S.; Hancock, R. D. *Inorg. Chem.* **2011**, *50*, 8348.
- (24) Zong, R. F.; Thummel, R. P. *J. Am. Chem. Soc.* **2004**, *126*, 10800.
- (25) Cockrell, G. M.; Zhang, G.; VanDerveer, D. G.; Thummel, R. P.; Hancock, R. D. *J. Am. Chem. Soc.* **2008**, *130*, 1420.
- (26) Carolan, A. N.; Mroz, A. E.; El Ojaimi, M.; VanDerveer, D. G.; Thummel, R. P.; Hancock, R. D. *Inorg. Chem.* **2012**, *51*, 3007.
- (27) Carolan, A. N.; Cockrell, G. M.; Williams, N. J.; Zhang, G.; VanDerveer, D. G.; Lee, H. S.; Thummel, R. P.; Hancock, R. D. *Inorg. Chem.* **2013**, *52*, 15.
- (28) Benay, G.; Schurhammer, R.; Wipff, G. *Phys. Chem. Chem. Phys.* **2011**, *13*, 2922.
- (29) Lewis, F. W.; Harwood, L. M.; Hudson, M. J.; Drew, M. G. B.; Desreux, J. F.; Vidick, G.; Bouslimani, N.; Modolo, G.; Wilden, A.; Sypula, M.; Vu, T. H.; Simonin, J. P. *J. Am. Chem. Soc.* **2011**, *133*, 13093.
- (30) Lewis, F. W.; Hudson, M. J.; Harwood, L. M. *Synlett* **2011**, 2609.
- (31) Lewis, F. W.; Harwood, L. M.; Hudson, M. J.; Drew, M. G. B.; Wilden, A.; Sypula, M.; Modolo, G.; Vu, T.-H.; Simonin, J.-P.; Vidick, G.; Bouslimani, N.; Desreux, J. F. *Procedia Chem.* **2012**, *7*, 231.
- (32) Manna, D.; Ghanty, T. K. *Phys. Chem. Chem. Phys.* **2012**, *14*, 11060.
- (33) Galletta, M.; Scaravaggi, S.; Macerata, E.; Famulari, A.; Mele, A.; Panzeri, W.; Sansone, F.; Casnati, A.; Mariani, M. *Dalton Trans* **2013**, *42*, 16930.
- (34) Lewis, F. W.; Harwood, L. M.; Hudson, M. J.; Drew, M. G.; Hubscher-Bruder, V.; Videva, V.; Arnaud-Neu, F.; Stamberg, K.; Vyas, S. *Inorg. Chem.* **2013**, *52*, 4993.
- (35) Whittaker, D. M.; Griffiths, T. L.; Helliwell, M.; Swinburne, A. N.; Natrajan, L. S.; Lewis, F. W.; Harwood, L. M.; Parry, S. A.; Sharrad, C. A. *Inorg. Chem.* **2013**, *52*, 3429.
- (36) Galletta, M.; Scaravaggi, S.; Macerata, E.; Famulari, A.; Mele, A.; Panzeri, W.; Sansone, F.; Casnati, A.; Mariani, M. *Dalton Trans* **2013**, *42*, 16930.
- (37) Bisson, J.; Berthon, C.; Berthon, L.; Boubals, N.; Dubreuil, D.; Charbonnel, M. C. *Procedia Chem.* **2012**, *7*, 13.
- (38) Xiao, C. L.; Wang, C. Z.; Yuan, L. Y.; Li, B.; He, H.; Wang, S.; Zhao, Y. L.; Chai, Z. F.; Shi, W. Q. *Inorg. Chem.* **2014**, *53*, 1712.
- (39) Frisch, M. J. et al. *Gaussian 09*, revision A.1; Gaussian, Inc.: Wallingford, CT, 2009.
- (40) Becke, A. D. *Phys. Rev. A* **1988**, *38*, 3098.
- (41) Lee, C. T.; Yang, W. T.; Parr, R. G. *Phys. Rev. B* **1988**, *37*, 785.
- (42) Dolg, M.; Stoll, H.; Preuss, H. *J. Chem. Phys.* **1989**, *90*, 1730.
- (43) Küchle, W.; Dolg, M.; Stoll, H.; Preuss, H. *J. Chem. Phys.* **1994**, *100*, 7535.
- (44) Cao, X. Y.; Dolg, M. *THEOCHEM* **2004**, *673*, 203.
- (45) Lan, J. H.; Shi, W. Q.; Yuan, L. Y.; Zhao, Y. L.; Li, J.; Chai, Z. F. *Inorg. Chem.* **2011**, *50*, 9230.
- (46) Lan, J. H.; Shi, W. Q.; Yuan, L. Y.; Feng, Y. X.; Zhao, Y. L.; Chai, Z. F. *J. Phys. Chem. A* **2012**, *116*, 504.
- (47) Lan, J. H.; Shi, W. Q.; Yuan, L. Y.; Li, J.; Zhao, Y. L.; Chai, Z. F. *Coord. Chem. Rev.* **2012**, *256*, 1406.
- (48) Wang, C. Z.; Lan, J. H.; Zhao, Y. L.; Chai, Z. F.; Wei, Y. Z.; Shi, W. Q. *Inorg. Chem.* **2013**, *52*, 196.
- (49) Wang, C. Z.; Shi, W. Q.; Lan, J. H.; Zhao, Y. L.; Wei, Y. Z.; Chai, Z. F. *Inorg. Chem.* **2013**, *52*, 10904.
- (50) Wiberg, K. B. *Tetrahedron* **1968**, *24*, 1083.
- (51) Carpenter, J. E.; Weinhold, F. *THEOCHEM* **1988**, *46*, 41.
- (52) Reed, A. E.; Curtiss, L. A.; Weinhold, F. *Chem. Rev.* **1988**, *88*, 899.
- (53) Klamt, A.; Schüürmann, G. *J. Chem. Soc., Perkin Trans. 2* **1993**, 799.
- (54) Shamov, G. A.; Schreckenbach, G.; Martin, R. L.; Hay, P. J. *Inorg. Chem.* **2008**, *47*, 1465.
- (55) Shamov, G. A.; Schreckenbach, G. *J. Phys. Chem. A* **2005**, *109*, 10961.
- (56) Allen, P. G.; Bucher, J. J.; Shuh, D. K.; Edelstein, N. M.; Reich, T. *Inorg. Chem.* **1997**, *36*, 4676.
- (57) Hughes, K. A.; Burns, P. C. *Acta Crystallogr., Sect. C* **2003**, *59*, I7.
- (58) Gaunt, A. J.; May, I.; Neu, M. P.; Reilly, S. D.; Scott, B. L. *Inorg. Chem.* **2011**, *50*, 4244.
- (59) Conradson, S. D.; Abney, K. D.; Begg, B. D.; Brady, E. D.; Clark, D. L.; den Auwer, C.; Ding, M.; Dorhout, P. K.; Espinosa-Faller, F. J.; Gordon, P. L.; Haire, R. G.; Hess, N. J.; Hess, R. F.; Keogh, D. W.; Lander, G. H.; Lupinetti, A. J.; Morales, L. A.; Neu, M. P.; Palmer, P. D.; Paviet-Hartmann, P.; Reilly, S. D.; Runde, W. H.; Tait, C. D.; Veirs, D. K.; Wastin, F. *Inorg. Chem.* **2004**, *43*, 116.
- (60) Allen, P. G.; Veirs, D. K.; Conradson, S. D.; Smith, C. A.; Marsh, S. F. *Inorg. Chem.* **1996**, *35*, 2841.
- (61) Marie, C.; Miguiriditchian, M.; Guillaumont, D.; Tosseng, A.; Berthon, C.; Guilbaud, P.; Duvail, M.; Bisson, J.; Guillauneux, D.; Pipelier, M.; Dubreuil, D. *Inorg. Chem.* **2011**, *50*, 6557.
- (62) Marie, C.; Miguiriditchian, M.; Guillauneux, D.; Bisson, J.; Pipelier, M.; Dubreuil, D. *Solvent Extr. Ion Exch.* **2011**, *29*, 292.
- (63) Cao, X.; Heidelberg, D.; Ciupka, J.; Dolg, M. *Inorg. Chem.* **2010**, *49*, 10307.
- (64) Lapka, J. L.; Paulenova, A.; Alyapyshev, M. Y.; Babain, V. A.; Law, J. D.; Herbst, R. S. *IOP Conf. Ser.: Mater. Sci. Eng.* **2010**, *9*.